In-situ Electric Field for Human Body Model with Different Postures for Wireless Power Transfer System in an Electrical Vehicle

Takuya Shimamoto, Ilkka Laakso and Akimasa Hirata

Corresponding author:

Akimasa Hirata

Nagoya Institute of Technology

ahirata@nitech.ac.jp

Abstract

In-situ electric field of an adult male model in different postures is evaluated for the magnetic field leaked from a wireless power transfer system in an electrical vehicle. The transfer system is implemented below the centre of the vehicle body and the transferred power and frequency are 7 kW (peak) and 85 kHz. The in-situ electric field is evaluated for the human models (i) crouching near the vehicle, (ii) lying on the ground with or without his arm stretched, (iii) sitting on the driver's seat, and (iv) standing on a transmitting coil without a receiving coil. In each scenario, the in-situ electric fields are smaller than the allowable limit prescribed in international guidelines, although the magnetic field strength in the human body is locally higher than the allowable external magnetic field strength. The highest in-situ electric field was observed when the human lies on the ground with his arm extended toward the coils because of higher magnetic field around the arm.

1. Introduction

With the progress of wireless power transfer (WPT) technology, the transferred power and distance are expected to increase. One of the most promising and high-power applications of WPT is to charge electrical vehicles (Shinohara, 2011). Several tests for charging electrical vehicles including busses have been conducted extensively over the world (Ichikawa *et al.*, 2013; Showa Aircraft Industry Co.; Tell *et al.*, 2014). The maximum transmitting power for charging vehicles is expected to be several kilowatts or higher (Ichikawa *et al.*, 2013; Tell *et al.*, 2014); 7 kW (peak) in Japan. The magnetic field leaked from a WPT system implemented under the vehicle body is highly nonuniform (Ichikawa *et al.*, 2013) and its spatiotemporal maximum exceeds the reference level or maximal allowable field strength prescribed in the international guidelines (Laakso and Hirata, 2013); the compliance in terms of the external magnetic field is rather conservative for non-uniform exposure. Under such a circumstances, compliance with the basic restrictions or the allowable in-situ electric field (< 100 kHz) is needed (Laakso *et al.*, 2012; Christ *et al.*, 2013; Park *et al.*, 2013; Chen *et al.*, 2014).

In our previous study (Laakso and Hirata, 2013), the in-situ electric field was evaluated in adult and child models in a standing posture for a typical WPT system for an electrical vehicle. Computational results showed that the in-situ field was well within the basic restrictions although the magnetic field strength around the feet and lower legs violated the reference level. Another concern for this application is if the in-situ electric field limit is satisfied even for different postures, e.g. fora person crouching or lying on the ground next to the vehicle, which may increase the strength of the magnetic field in the body. The effect of posture on induced physical quantities has previously been investigated for clarifying the relationship between the basic restriction and reference level at frequencies higher than 10 MHz (Findlay and Dimbylow, 2005; Nagaoka and Watanabe, 2009; Uusitupa *et al.*, 2010), but there are so far little data about the effects of posture for non-uniform exposure at lower frequencies.

The purpose of this study is to conduct electromagnetic dosimetry of an adult male model in different postures for the magnetic field leaked from a WPT system implemented in an electric vehicle. Note that the in-situ electric fields in children are expected to be smaller than those in adults because of smaller cross-sectional area of the body (Laakso and Hirata, 2013; Kos *et al.*, 2012).

2. Model and methods

2.1. Modelling vehicle and resonant coils

Figure 1 illustrates the geometry of a vehicle with a wireless power transfer system consisting of two resonant coils. The vehicle body, whose dimensions are approximately equal to a commercially available vehicle, is modelled as a perfect conductor. The specifications of the coils are as follows: the transmitting and receiving coils are identical with (i) a separation of 120 mm, (ii) a rectangular

core with a size of 325 mm × 405 mm, and (iii) 14 turns. The coils are also modelled as perfectly conducting wires. The transfer frequency was chosen as 85 kHz. The transmitting power was set as 7 kW (peak), which is approximately the maximum one considered for wireless vehicle charging in Japan. The coils are implemented below the centre of the vehicle body, which is one of the promising positions under consideration. Note that the coil was implemented below the rear of the vehicle body in our previous study (Laakso and Hirata, 2013). The most notable difference between these two coil positions is that the distance between the coils has been changed from 150 mm to 120 mm due to different separations between the ground and the vehicle body.

The coils are assumed to be misaligned by 200 mm in the side-to-side direction and 100 mm in front-to-back direction (Ichikawa *et al.*, 2013), as shown in figure 1. The magnetic field leaked from the vehicle in this case is larger than that in the case where the coils are exactly aligned, corresponding to the exposure scenario of the worst case. Note that experimental validation for our coil modeling has been presented in our previous study by comparing measured magnetic field distribution (Laakso and Hirata, 2013).

2.2. Human body models

The MRI-based whole-body voxel model named TARO was considered in this study (Nagaoka *et al.*, 2004). This model has a resolution of 2 mm × 2 mm × 2 mm and is segmented into 51 anatomical tissues/organs. The conductivities of tissues were taken from the database by Gabriel *et al.* (1996). In this study, the conductivity of the skin was set to be that of wet skin, which is slightly higher than that of subcutaneous fat at the studied frequency. Note that the role of skin conductivity has been discussed extensively by Schmid *et al.* (2013) suggesting that Gabriel's model underestimate the conductivity of skin by a large margin.

To realize different postures of the model, free software provided by National Institute of Information and Communications Technology, was used (Nagaoka and Watanabe, 2009).

2.3. Computational methods

The computational procedure is identical to that in our previous study (Laakso and Hirata, 2013). Because the transfer frequency was 85 kHz, the magneto-quasi-static approximation was applicable; this approximation has been shown to be valid for power transfer at frequencies up to 10 MHz at least for localized exposure (Hirata *et al.*, 2013). Under the approximation, the electric displacement current is ignored, and the induced currents in the human body are assumed not to perturb the external magnetic field.

The resonant coils and the magnetic field distribution around the vehicle without the human body model were modelled with commercial software HFSS (ANSYS, Inc.), which utilizes the full-wave finite-element method (FEM). The magnetic fields in several rectangular volumes, which would be

occupied by the human body, were extracted from HFSS in grids with a resolution of 50 mm × 50 mm × 50 mm. These data were used to construct a magnetic vector potential that gave approximately the same magnetic field and was defined in a grid with a resolution of 2 mm × 2 mm × 2 mm. The electric fields induced in the human body by the magnetic vector potential were then determined using a different in-house magneto-quasistatic FEM solver. The FEM solver utilizes piecewise linear basis functions and has been described in detail in Laakso *et al.* (2012). The elements were cubical with a side length of 2 mm, and each element corresponded to one voxel. As described in Laakso *et al.* (2012), the FEM linear equation system was solved iteratively using the geometric multigrid method. The number of multigrid levels was six, and the iteration was continued until the relative residual was less than 10^{-9}.

2.4. Exposure scenario and Dose metric

As exposure scenarios, following four cases were considered: a human body model (i) crouching near the side of the vehicle, (ii) lying on the ground with or without its right arm stretched toward the coils, (iii) sitting on the driver's seat, in addition that (iv) the human body stands on the primary coil without considering the receiving coil (waiting condition). A detailed definition of the position of the human body relative to the vehicle body will be presented in the Results section. Note that in scenario (ii), the human body is not located under the vehicle body except for the arm because the separation between the vehicle body and the ground is 200 mm, which is smaller than the depth of the human body model. In scenario (iii), the windows of the vehicle are considered while the dashboard, seats, etc. are not modelled. A human model with a realistic posture was developed based on the ISO standard (???) and then put in the corresponding position of the driver's seat. In scenarios (i), (II), and (iii), the transmitting power is 7 kW (peak) while it is 5 W (peak) in scenario (iv). The latter transmitting power has not been well defined at this moment, but it is expected to be much smaller than that in the charging condition. Thus, the transmitting power considered in our previous study for different application is considered (Sunohara *et al.*, 2014). Note that the in-situ electric fields are proportional to the square root of the transmitting power.

The 99th percentile value of an induced electric field is suggested for use in international guidelines (ICNIRP, 2010). The rationale for this metric is based on computations using a spherical model exposed to a uniform magnetic field. In such a scenario, the computationally derived maximal induced electric field is stronger than the analytic maximum value by several dozen percent because of numerical staircasing errors. In our previous study, less than 0.5% of the voxels have notable staircasing error, even for uniform exposure (Hirata *et al.*, 2011). The 99.9th percentile value of the induced electric field is used as a dose metric from the standpoint of conservativeness for non-uniform exposures (Laakso and Hirata, 2013; Kos *et al.*, 2012).

3. Computational results

3.1. Magnetic field distribution around vehicle

Figure 2 illustrates the magnetic field distribution around the vehicle. Note that the region where the reference level for the general public is not satisfied is represented in red. As shown in figure 2, the amplitude and direction of the magnetic field vary spatially. The maximum value of the magnetic field excluding the region under the vehicle was 56.7 A m^{-1}, which is larger than the reference level of 21 A m^{-1}. Note that this maximum value is smaller than that in our previous study where the receiving coil was implemented in the rear of the vehicle body. The main reason for this difference is attributable to the separation of the vehicle body and ground; it was 300 mm for the rear while 200 mm for the centre. The computed transfer efficiency between the coils was 97.1% at that time.

3.2. Variation of induced electric field in human body model with different posture

3.2.1. In-situ electric field in the human model standing near the vehicle

The dependence of the 99.9th percentile value of in-situ electric field on the separation between the standing human model and the vehicle body was computed (see figure 2 (a)). The separation was defined as the distance from the body to the closest part of the body (toes); the distance from the chest is 40 mm. In this computation, the position of the human body in the front-to-rear direction is chosen so that the 99.9th percentile value of in-situ electric field becomes maximal when the model is moved in the rear-to-front direction. As shown in figure 3, the in-situ electric field decreases exponentially with the increase of the separation. At the distance 0, the 99.9th percentile value of in-situ electric field was 0.40 V m^{-1} which appeared around the ankle.

3.2.2. In-situ electric field in the human model with different postures

Figure 4 illustrates the in-situ electric field in the model crouching around the vehicle. The separation between the tip of the fingers and the vehicle body was set to zero. The 99.9th percentile value of the in-situ electric field is 0.92 V m^{-1}, which is 2.3 times larger than that in the standing posture. As shown in figure 4, the in-situ electric field becomes large in the thigh whose cross sectional area is larger than that of the ankle. Note that the effective magnetic flux passing through the human body is essential to estimate the in-situ electric field (Laakso *et al.*, 2012).

Figure 5 illustrates the in-situ electric field in the model lying on the ground. The models with and without the arm stretched are considered. In this scenario, the separation between the closest body part (right thigh) excluding the right arm and shoulder and the vehicle is zero. Thus, a part of the shoulder is under the vehicle body for the model without the stretch of the arm. The in-situ electric field for the model with and without the arm stretched are 5.95 V m^{-1} and 2.30 V m^{-1}, respectively. For the case where the separation between the right shoulder and vehicle body is zero, the in-situ electric field was 2.83 V m^{-1}.

3.2.3. Human model sitting on the driver's seat.

Figure 6 shows the in-situ electric field distribution of the human model sitting on the driver's seat. As seen from figure 6, the in-situ electric field becomes large at the buttocks. This hot spot is caused by larger cross sectional area of the buttocks and non-uniform magnetic field leaked in from the window. The 99.9^{th} percentile value of the in-situ electric field was 0.024 V m^{-1}.

3.2.4. Human model standing on transmitting coil.

Figure 7 shows the in-situ electric field distribution of the human model standing on the transmitting coil. The in-situ electric field is the largest around the feet. The in-situ electric field in the remaining part is much smaller than that in the feet. The 99.9^{th} percentile value of the in-situ electric field was 0.549 V m^{-1}.

4. Discussion and Summary

The IEC has published two standards for product safety in part related to the exposure scenario in an electrical vehicle. One is IEC 62233 (2005) in which household appliances are considered for frequencies ranging from 10 Hz to 400 kHz. The other is IEC 62110 (2009), in which an AC power system is considered at power frequencies (50 and 60 Hz). The distance between the product and the human body is defined as 30 cm and 20 cm, respectively, in the above standards. Our previous study demonstrated that even for the standing posture with the distance of 0 cm the in-situ electric field is satisfied with the basic restriction. As is similar to the systems in IEC 62233 and 62110, the electrical vehicle may be charged in public space. Thus, a human body model with realistic postures under realistic environments was considered for further confirmation. In the scenarios considered, the distance between the wireless power transfer system and the human body was smaller than the distance defined in the conventional IEC standards. For all the cases considered herein, the 99.9^{th} percentile value of the in-situ electric field, a conservative surrogate of 99^{th} percentile prescribed in the guidelines for non-uniform exposure, is smaller than the basic restriction prescribed in the ICNIRP guidelines.

The in-situ electric fields were found to be strongly affected by the posture. The closer the human body was to the ground level, where the magnetic field was the highest, the stronger were the induced in-situ electric fields. Crouching posture increased the in situ electric field by a factor 2.3 compared to the standing posture, and the fields were further increased if the model was lying on the ground without or with the arm extended towards the coils (factors of 2.5 and 6.5). Additional exposure scenarios of the human body model sitting on the driver's seat and standing on the transmitting coil without the receiving coil were investigated. The induced electric fields were found to be one order of magnitude smaller than those in the case of the model standing by the side of the

vehicle.

The largest in-situ electric field (5.95 V m^{-1}) was observed in the model lying on the ground with the arm extended toward the resonant coils. At that time, the magnetic field averaged over the region where the arm exists was 382 A m^{-1}, which was 18 times higher than the reference level of 21 A m^{-1}. The reason why the in-situ electric field complies with the basic restriction for such a large external *magnetic field* is attributable to the relatively small *magnetic flux* passing through the arm with a cross sectional area much smaller than that of the human trunk or the whole body. Additionally, the reference level has been set to be conservative for uniform whole-body exposure with an added "dosimetric uncertainty factor" of three (ICNIRP 2010).

In summary, the body posture may have a considerable effect on the in situ electric fields, and there are difficulties in applying the magnetic-field reference levels to non-uniform exposure. It remains up for discussion if and how the potential effects of posture should be considered in the safety standardization of wireless electric vehicle charging systems.

References

Chen X L, Umenei A E, Baarman D W, Chavannes N, De Santis V, Mosig J R and Kuster N 2014 Human exposure to close-range resonant wireless power transfer systems as a function of design parameters

Christ A, Douglas M, Nadakuduti J and Kuster N 2013 Assessing human exposure to electromagnetic fields from wireless power transmission systems *Proc. IEEE* **101** 1482-93

Findlay R and Dimbylow P 2005 Effects of posture on FDTD calculations of specific absorption rate in a voxel model of the human body *Physics in Medicine and Biology* **50** 3825

Gabriel S, Lau R W and Gabriel C 1996 The dielectric properties of biological tissues: III. Parametric models for the dielectric spectrum of tissues *Phys. Med. Biol.* **41** 2271

Hirata A, Ito F and Laakso I 2013 Confirmation of quasi-static approximation in SAR evaluation for a wireless power transfer system *Physics in Medicine and Biology* **58** N241

Hirata A, Takano Y, Fujiwara O, Dovan T and Kavet R 2011 An electric field induced in the retina and brain at threshold magnetic flux density causing magnetophosphenes *Phys. Med. Biol.* **56** 4091-101

Ichikawa S, Mori A and Kawakubo A 2013 Development of short range wireless power transfer test system using magnetic resonance (3) magnetic field characteristic of a kW-class system using solenoid coils *Proc. IEICE Society Conf. (in Japanese)*

ICNIRP 2010 Guidelines for limiting exposure to time-varying electric and magnetic fields (1 Hz to 100 kHz) *Health Physics* **99** 818-36

Kos B, Valič B, Kotnik T and Gajšek P 2012 Occupational exposure assessment of magnetic fields generated by induction heating equipment—the role of spatial averaging *Physics in Medicine and Biology* **57** 5943

Laakso I and Hirata A 2013 Evaluation of the induced electric field and compliance procedure for a wireless power transfer system in an electrical vehicle *Physics in Medicine and Biology* **58** 7583

Laakso I, Tsuchida S, Hirata A and Kamimura Y 2012 Evaluation of SAR in a human body model due to wireless power transmission in the 10 MHz band *Phys. Med. Biol.* **57** 4991

Nagaoka T and Watanabe S 2009 Voxel-based variable posture models of human anatomy *Proceedings of the IEEE* **97** 2015-25

Nagaoka T, Watanabe S, Sakurai K, Kunieda E, Taki M and Yamanaka Y 2004 Development of realistic high-resolution whole-body voxel models of Japanese adult males and females of average height and weight, and application of models to radio-frequency electromagnetic-field dosimetry *Phys. Med. Biol.* **49** 1-15

Park P, Wake K and Watanabe S 2013 Incident Electric Field Effect and Numerical Dosimetry for a Wireless Power Transfer System Using Magnetically Coupled Resonances *Microwave Theory and Techniques, IEEE Transactions on* **61** 3461-9

Schmid G, Cecil S and Überbacher R 2013 The role of skin conductivity in a low frequency exposure assessment for peripheral nerve tissue according to the ICNIRP 2010 guidelines *Physics in Medicine and Biology* **58** 4703

Shinohara N 2011 Power without wires *Microwave Magazine, IEEE* **12** S64-S73

Showa Aircraft Industry Co. L Wireless Power Supply, http://www.showa-aircraft.co.jp/products/EV/kyuuden.html

Sunohara T, Hirata A, Laakso I and Onishi T 2014 Analysis of in situ electric field and specific absorption rate in human models for wireless power transfer system with induction coupling *Physics in Medicine and Biology* **59** 3721

Tell R, Kavet R, Bailey J and Halliwell J 2014 Very-low-frequency and low-frequency electric and magnetic fields associated with electric shuttle bus wireless charging *Radiation Protection Dosimetry* **158** 123-34

Uusitupa T, Laakso I, Ilvonen S and Nikoskinen K 2010 SAR variation study from 300 to 5000 MHz for 15 voxel models including different postures *Physics in Medicine and Biology* **55** 1157

Captions

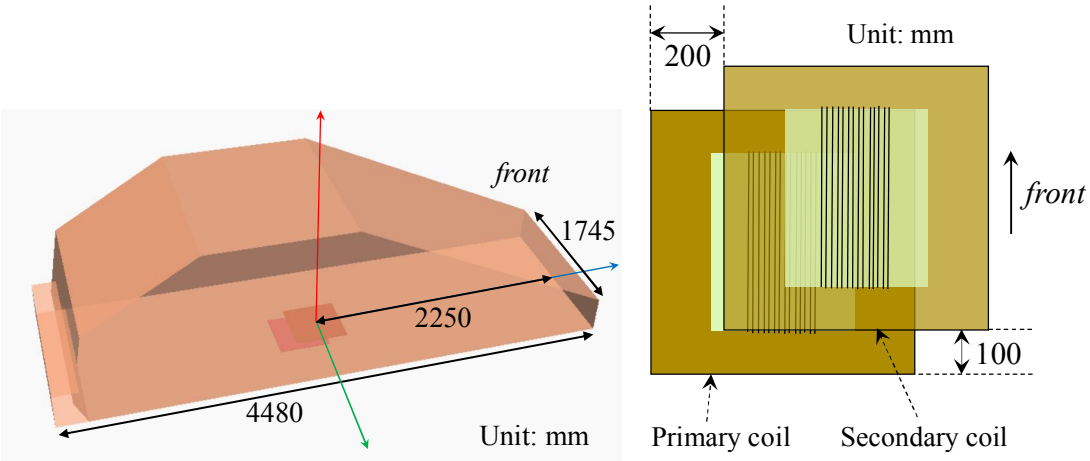

(a) (b)

Figure 1. (a) Bird view of an electrical vehicle with a wireless power transfer system and (b) schematic explanation of misalignment of two coils.

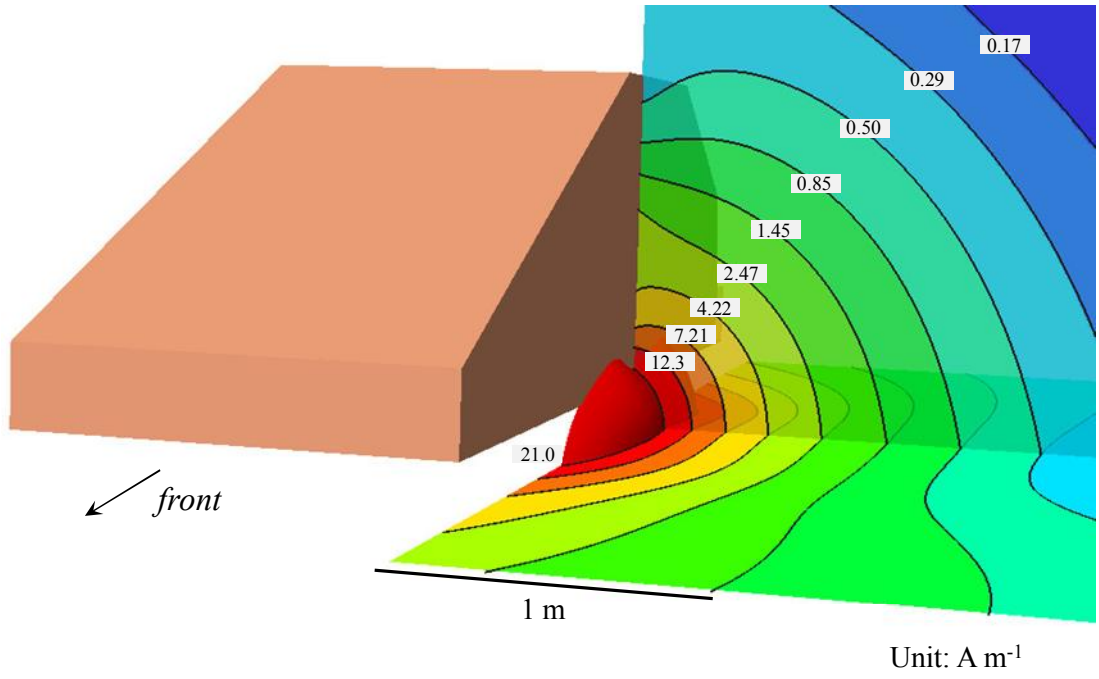

Figure 2. The magnetic field distribution from the wireless power transfer system. Streamlines represent the direction, and the contours represent the strength of the magnetic field. The solid red region is the volume where the strength of the magnetic field exceeds the ICNIRP reference level for the general public.

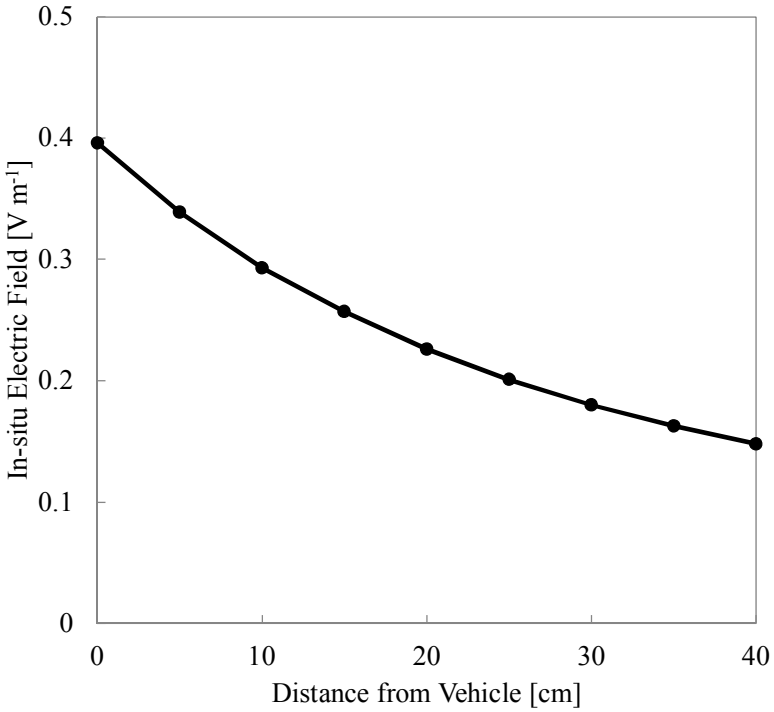

Figure 3. The dependence of the maximum in-situ electric field in a standing human body.

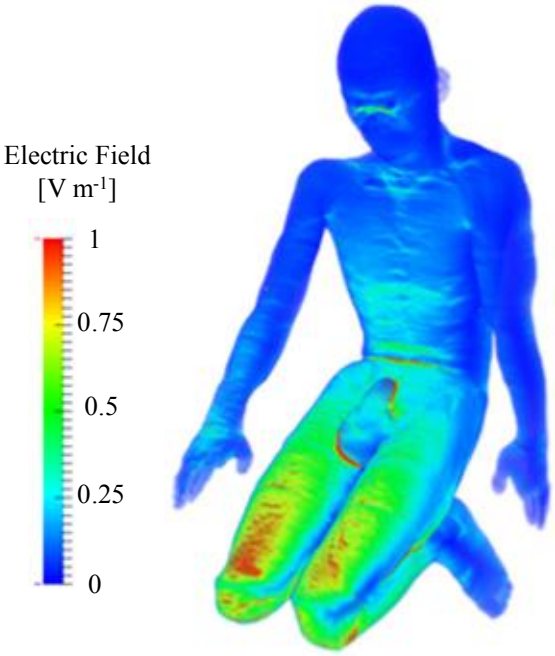

Figure 4. The in-situ electric field distribution in the human model with crouching posture.

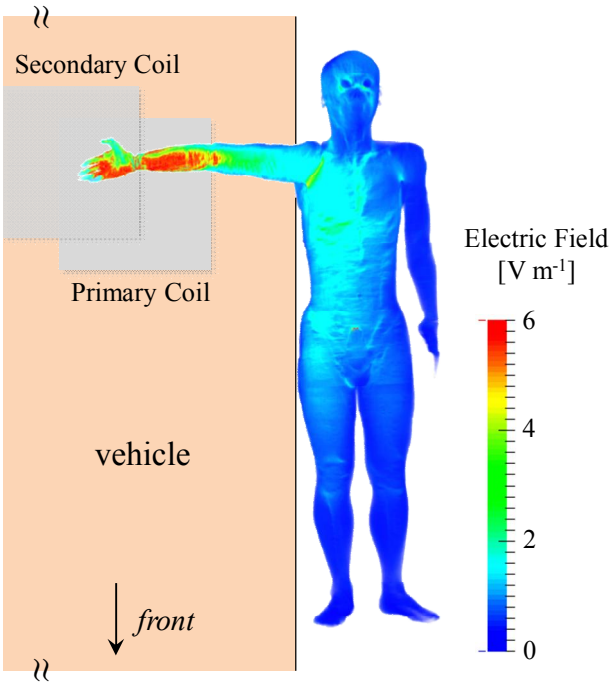

Figure 5. The in-situ electric field distributions in a human body model lying on the ground (a) with and (b) without his right arm stretched.

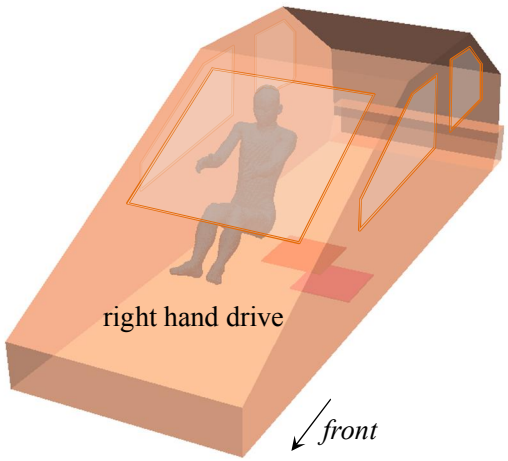

(a)

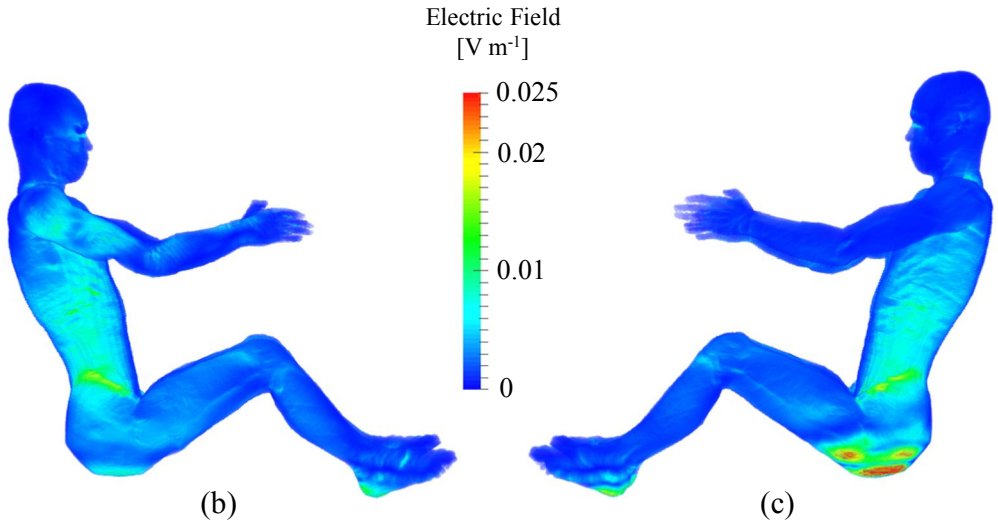

Figure 6. The in-situ electric field distributions in the human model with a sitting posture in the driver's seat: (a) birdview of the vehicle body with the driver, views from (b) right-hand and (c) left-hand sides.

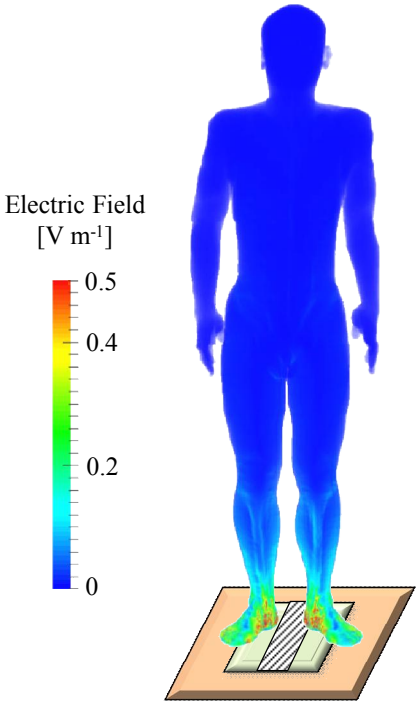

Figure 7. The in-situ electric field distribution in the human model standing on the transmitting coil without the receiving coil.